ELSEVIER

Journal of Photochemistry and Photobiology A: Chemistry 139 (2001) 53–62

Journal of Photochemistry and Photobiology A:Chemistry

www.elsevier.nl/locate/jphotochem

Site selectivity in excited-state intramolecular proton transfer in flavonols

N.A. Nemkovich [a,*], J.V. Kruchenok [a], A.N. Rubinov [a], V.G. Pivovarenko [b], W. Baumann [c]

[a] *B.I. Stepanov Institute of Physics, National Academy of Sciences of Belarus, F. Skaryna Avenue 68, 220072 Minsk, Belarus*
[b] *Department of Chemistry, National Taras Shevchenko University, Volodymyrska 64, 252033 Kiev, Ukraine*
[c] *Institute of Physical Chemistry, University of Mainz, Jakob Welder-Weg 11, 55099 Mainz, Germany*

Received 9 March 2000; received in revised form 29 October 2000; accepted 29 October 2000

Abstract

To investigate 4′-(diethylamino) (FET) and 4′-*N*-(15-azacrown-5) (FCR) derivatives of 3-hydroxyflavone in binary solvents and erythrocyte ghosts, we used the red-edge excitation spectroscopy (REES). The results obtained prove the existence of spectral heterogeneity of flavonols in the studied systems. The effect manifests itself in the dependence of the efficiency of excited-state intramolecular proton transfer (ESIPT) on the excitation frequency. The electro-optical absorption method (EOAM) was used to measure the dipole moments of the normal form of FET. The electric dipole moments in the ground ($\boldsymbol{\mu}_g$) and excited Franck–Condon ($\boldsymbol{\mu}_e^{FC}$) states have the values 22.7×10^{-30} and 53.3×10^{-30} C m, respectively. On optical excitation, the electric dipole moment increases by 34×10^{-30} C m, and the angle between $\boldsymbol{\mu}_g$ and $\boldsymbol{\mu}_e^{FC}$ is 25°. The results of the electro-optical and spectroscopic measurements enable us to describe more precisely the process of charge and proton transfer in 4′-amino-3-hydroxyflavones. Charge transfer and proton transfer occur alternately. The main stage of forward electron charge transfer takes place after excitation of the normal form (N*) and partly after ESIPT. In the phototautomer (T), only partial reverse charge transfer happens after photon emission. The second, more efficient stage of reverse electron charge transfer occurs after radiationless conversion of phototautomer into the normal form.

Keywords: Flavonols; Fluorescent probes; Binary solvents; Biological membranes; Red-edge excitation

1. Introduction

The basic mechanism of operation of the most widely used dipolar fluorescent probes is their spectroscopic response to the local dielectric constant (more exactly, dielectric interactions) and dipole-reorientational dynamics of the surrounding molecules. For this purpose, a series of derivatives of naphthalenes, anthracenes, phthalimides, etc. with substituted polar groups has been synthesized [1,2]. These molecules demonstrate a significant charge separation in the excited state, which in many cases can be stabilized by geometrical changes in the probe molecule (e.g., twisted intramolecular charge transfer [3]). Investigation of these probes has made it possible to observe strongly pronounced and extremely interesting spectroscopic phenomena: time-dependent fluorescence Stokes shift [4–6], static and dynamic inhomogeneous broadening of electronic spectra [7] and such "red-edge excitation" effects [8] related with these phenomena as dispersive electronic excitation energy transport [9,10], wavelength-dependent rotation of probe molecules [11], etc. These phenomena are successfully used in the studies of structural changes and molecular dynamics in solutions and biological systems. Further progress in this field can be achieved on the basis of development of new probes operating on novel principles of the spectroscopic response and the use of modern laser methods. Very attractive in this respect are the 4′-amino derivatives of 3-hydroxyflavone as new fluorescent probes based on a coupling of ICT with excited-state intramolecular proton transfer (ESIPT). The spectra observed in various solvents have two well-resolved fluorescence bands, one of which corresponds to the emission of the normal form (N*), and the other one to the flavonol phototautomer (T*). As shown in Refs. [12–16], the ICT effect can be used for sensing the polarity, dielectric relaxation rate, and electric field gradient in a system, whereas the coupling with ESIPT must provide an enhanced spectral shift. Due to the interplay between the intramolecular charge and proton transfer in these flavonol derivatives [12–14], new photophysical phenomena should be observed when the methods

Abbreviations: FET, 4′-(diethylamino)-3-hydroxyflavone; FCR, 4′-*N*-(15-azacrown-5)-3-hydroxyflavone; ESIPT, excited-state intramolecular proton transfer; GSIPT, ground-state intramolecular proton transfer; ICT, intramolecular charge transfer; EOAM, electro-optical absorption method; REES, red-edge excitation spectroscopy; DMSO, dimethylsulfoxide; PMR, proton magnetic resonance

*Corresponding author. Fax: +375-17-2841646.
E-mail address: nemkov@dragon.bas-net.by (N.A. Nemkovich).

1010-6030/01/$ – see front matter
PII: S1010-6030(00)00408-1

of site-selective time-resolved laser spectroscopy are used.

In this paper, we describe the red-edge excitation effects for two novel flavonols in binary solvents and biological membranes, which have never been previously observed for proton-transfer reactions. The proposed mechanism results from the inhomogeneous broadening of electronic spectra due to the distribution of interactions between the polar ICT state and the polar environment. Using selective excitation at the red edge of the absorption spectrum, probe molecules with stronger interactions with their environment can be selected. The probability of ESIPT in such elementary cells (solvates) differs from the probability of this process averaged over the bulk of solution. In addition, we have measured the dipole moments in the equilibrium ground and excited Franck–Condon states of one of the flavonols using the electro-optical absorption method (EOAM).

2. Experimental

2.1. Flavonol synthesis

The flavonols (Fig. 1) have been synthesized from 2-hydroxyacetophenone and the corresponding benzaldehydes by the Algar–Flynn–Oyamada reaction [17,18] and purified by means of repeated recrystallization or column chromatography. All flavonols were homogeneous according to thin-layer chromatography on Silufol UV-254 plates in chloroform–methanol (98:2, 95:5, 9:1 or 85:15 v/v) with following detection by UV excitation at 254 and 360 nm wavelengths. Their structures have been confirmed by quantitative elemental analysis, proton magnetic resonance (PMR), UV–visible and infrared (IR) spectrometry. PMR spectra were recorded on a Bruker CXP-200 Fourier spectrometer at room temperature with tetramethylsilane as internal standard. IR spectra were recorded in a Pye Unicam SP3-300 instrument in pellets of KBr. The basic physical–chemical characteristics of 4′-(diethylamino)-3-hydroxyflavone (FET) and 4′-*N*-(15-azacrown-5)-3-hydroxyflavone (FCR) correspond to those presented previously [15,16].

4'-(diethylamino)-3-hydroxyflavone (FET)

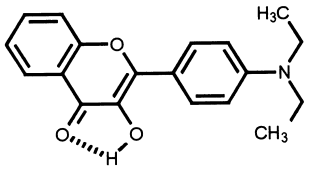

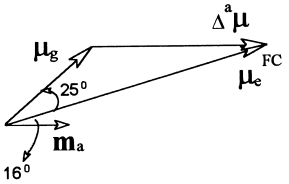

4'-N-(15-azacrown-5)-3-hydroxyflavone (FCR)

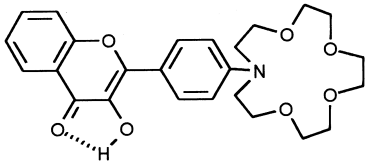

Fig. 1. Fluorescence probes studied in this work and diagram of different dipole moments of FET. The orientation of the transition dipole moment relative to the structural formula is arbitrary.

2.2. Other chemical procedures and sample preparation

All solvents and reagents were obtained from Merck and some of them were additionally purified by the methods described in Ref. [19]. The purified solvents were dried prior to use in the electro-optical measurements by distillation under reflux conditions with a sodium/potassium alloy employing an argon atmosphere. Purity of the solvents was checked by UV absorption measurements (1 cm cell; reference air).

The red blood cell membranes (hemoglobin-free ghosts of erythrocytes) were obtained from samples of human blood provided by the Research Institute of Blood, and Research Clinical Institute of Radiation Medicine and Endocrinology of the Ministry of Public Health of Belarus. We employed method of erythrocyte ghosts preparation originally described by Dodge [20].

2.3. Measurements

The steady-state absorption and emission spectra were recorded by a Cary 500 spectrophotometer and SFL-112A spectrofluorimeter, respectively.

To determine the ground- and excited-state dipole moments of the normal form, we used EOAM. Experimental details on the electro-optical methods have been reviewed extensively [3,21]. Using Liptay's [22] formalism, the effect of an external electric field E_f on the molar absorption coefficient $\kappa(\tilde{\nu})$ can be described by a quantity L, which is defined by

$$L = L(\tilde{\nu}, \chi) = \frac{\kappa^{E}(\tilde{\nu}, \chi) - \kappa(\tilde{\nu})}{\kappa(\tilde{\nu}) E_f^2} \quad (1)$$

where κ^E is the molar absorption coefficient in the presence of an applied electric field, κ the same without applied electric field, χ the angle between the direction of E_f and the electric field vector of the incident light, and $\tilde{\nu}$ the wavenumber. For a homogeneously broadened absorption band L is

given by the following equation:

$$L = Dr + \tfrac{1}{6}Es + Frt + Gst + Hru + Isu \quad (2)$$

where the parameters r and s are determined by the angle χ, and the quantities t and u depend on the first and second derivatives of the absorption spectrum:

$$r = \tfrac{1}{5}(2 - \cos^2\chi) \quad (3)$$

$$s = \tfrac{1}{5}(3\cos^2\chi - 1) \quad (4)$$

$$t = \frac{(1/hc)(\kappa/\tilde{\nu})^{-1}\,\mathrm{d}(\kappa/\tilde{\nu})}{\mathrm{d}\tilde{\nu}} \quad (5)$$

$$u = \frac{(1/2h^2c^2)(\kappa/\tilde{\nu})^{-1}\,\mathrm{d}^2(\kappa/\tilde{\nu})}{\mathrm{d}\tilde{\nu}^2} \quad (6)$$

For the molecules discussed in this communication, explicit polarizability and transition polarizability effects can be neglected compared with the electric dipole moment terms. Then the coefficients D, E, F, G, H, and I are as follows:

$$D = 0 \quad (7)$$

$$E = \left(\frac{1}{kT}\right)^2 f_e^2[3(\boldsymbol{m}_a\boldsymbol{\mu}_g) - \boldsymbol{\mu}_g^2] \quad (8)$$

$$F = \left(\frac{1}{kT}\right) f_e^2(\boldsymbol{\mu}_g\Delta^a\boldsymbol{\mu}) \quad (9)$$

$$G = \left(\frac{1}{kT}\right) f_e^2(\boldsymbol{m}_a\boldsymbol{\mu}_g)(\boldsymbol{m}_a\Delta^a\boldsymbol{\mu}) \quad (10)$$

$$H = f_e^2(\Delta^a\boldsymbol{\mu})^2 \quad (11)$$

$$I = f_e^2(\boldsymbol{m}_a\Delta^a\boldsymbol{\mu})^2 \quad (12)$$

where k is the Boltzmann constant, T the temperature, $\boldsymbol{m}_a$ the unit vector in the direction of the transition moment for absorption, $\boldsymbol{\mu}_g$ the dipole moment vector in the equilibrium ground state, and $\Delta^a\boldsymbol{\mu}$ the change of the dipole moment vector after transition to the excited Franck–Condon state. From a set of these five coefficients, the values of $\boldsymbol{\mu}_g$, $\Delta^a\boldsymbol{\mu}$ and the angles between the transition moments $\boldsymbol{m}_a$ and $\boldsymbol{\mu}_g$ and $\Delta^a\boldsymbol{\mu}$ can be determined. The cavity field correction f_e is defined according to Onsager's model as introduced to the electro-optical methods by Liptay [22]:

The quantity $L(\tilde{\nu}, \chi)$ in the present work was determined for two values of the angle χ ($\chi = 0$ and $\pi/2$) and for a set of wavenumbers within the first absorption band. Then the coefficients (8)–(12) and their standard deviations were obtained by multiple linear regression.

3. Results

3.1. Electronic spectra of FET and FCR in pure and binary solvents

Our studies on FET and FCR have demonstrated their high spectral sensitivity to such solvent characteristics as polarity. First of all, this sensitivity appears in the steady-state fluorescence spectra as different spectral position, intensity and width of the flavonol normal form (N*) and phototautomer (T*) emission bands. The fluorescence spectra of FET and FCR in various aprotic solvents are shown in Fig. 2. For FET and FCR, both the N* and T* forms display a positive solvatofluorochromic effect. Fig. 3 shows the dependence of the normal and phototautomer fluorescence peak frequencies for FET and FCR on the reaction field factor $F(\varepsilon, n)$ [21–23]. The frequency shift of the normal fluorescence peak ν_{em}^{max} is strongly dependent on the reaction field factor. For example, in the case of FCR, ν_{em}^{max} changes from 22 500 cm^{-1} in cyclohexane to 18 500 cm^{-1} in dimethylsulfoxide (DMSO) (Table 1). The relative intensity of the N* band as compared to the T* band changes dramatically from almost zero intensity in cyclohexane or decalin to more than 0.6 in DMSO. As follows from our measurements in polar aprotic solvents, the ratio of the I_{N^*}/I_{T^*} fluorescence peak intensities in polar aprotic solvents increases with increasing reaction field factor $F(\varepsilon, n)$ of the solvent (Table 1).

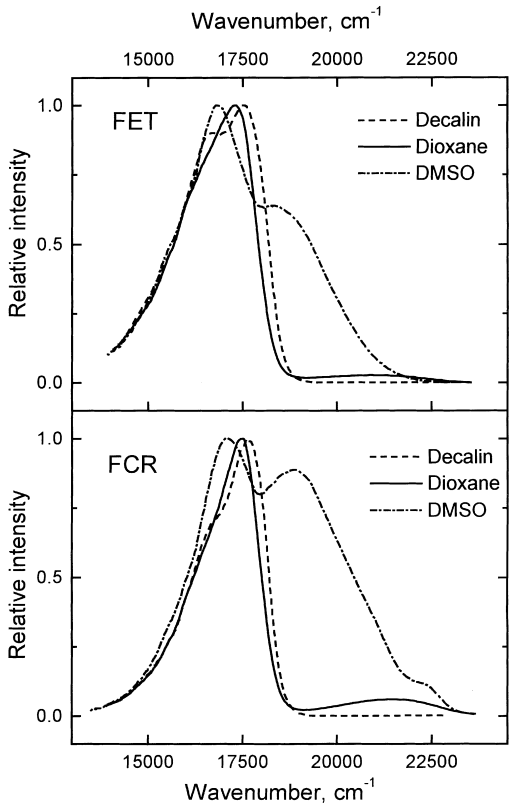

Fig. 2. Room temperature normalized fluorescence spectra of FET and FCR in aprotic solvents: decalin (– – –), dioxane (—), and DMSO (– – –).

The absorption maximum of FET and FCR shows a red shift with increasing solvent polarity. The excitation spectra of the probes recorded at the fluorescence maximum of both the normal and phototautomer forms in the solutions and erythrocyte ghosts are practically identical with each other and very similar to the absorption spectra.

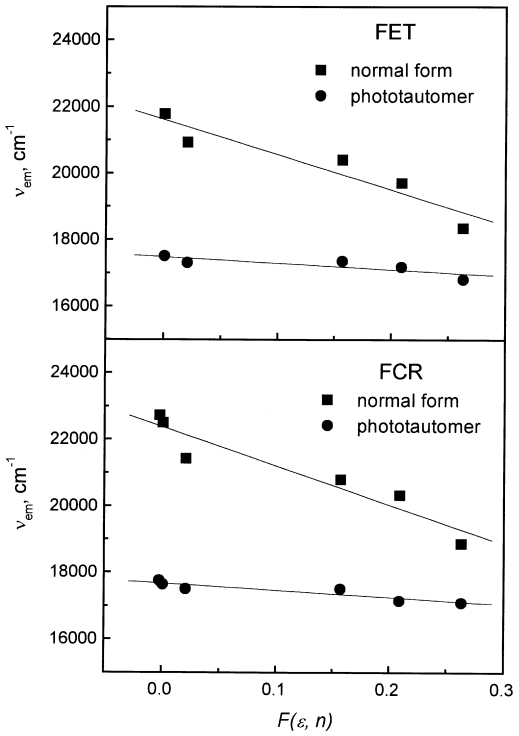

Fig. 3. Dependence of the normal (■) and phototautomer (●) fluorescence peak frequencies for FET and FCR as a function of the reaction field factor [23]: $F(\varepsilon, n) = (\varepsilon - 1)/(2\varepsilon + 1) - (n^2 - 1)/(2n^2 + 1)$, where ε is the relative permittivity of the solvent and n the refractive index. The values of $F(\varepsilon, n)$ are listed in Table 1.

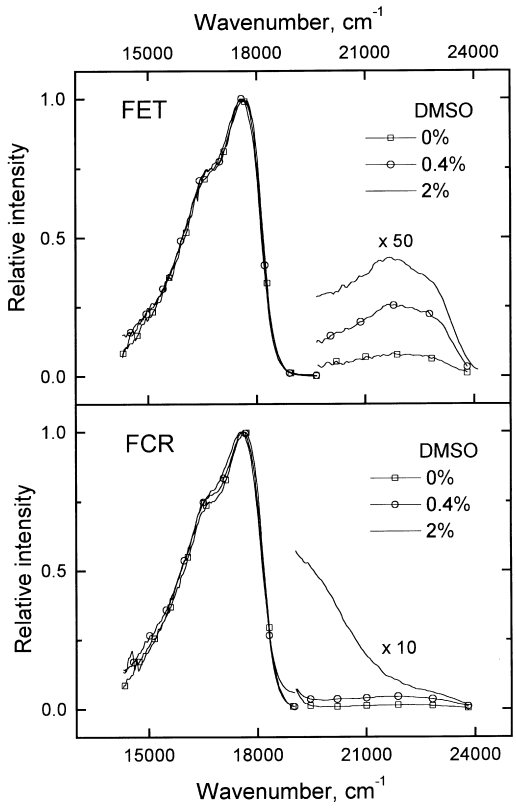

Fig. 4. Room temperature normalized fluorescence spectra of FET and FCR in decalin with varying volume concentrations of DMSO: 0% (–□–), 0.4% (–○–), and 2% (—). The emission spectrum of the normal form of FET and FCR expanded 50 and 10 times, respectively. The excitation frequency corresponds to the maximum of the absorption spectra.

We have found that the addition of DMSO to neutral solutions of FET and FCR in decalin and paraffin oil leads to a significant increase in the fluorescence intensity of the normal form (Fig. 4).

3.2. Red-edge excitation effects in binary solvents and erythrocyte ghosts

To investigate flavonols in binary solvents and erythrocyte ghosts, we used the red-edge excitation spectroscopy (REES) [7,8]. We have discovered that in binary solvents, the ratio I_{N^*}/I_{T^*} depends on the excitation frequency in all the cases (different concentrations and types of polar additives). As the excitation frequency is shifted to the red slope of the absorption spectrum, the fluorescence intensity of the form N^* increases monotonically with respect to that of the form T^*, and the red shift of both emission bands is observed. The normalized fluorescence spectra of FET and FCR in the mixture of decalin with DMSO obtained at excitation by various frequencies at the red edge of the absorption spectrum are shown in Fig. 5.

Table 1
Ratio (I_{N^*}/I_{T^*}) of the fluorescence peak intensities and the frequency of the fluorescence peak (ν_{em}^{max}) of different forms of flavonols in various solvents. $F(\varepsilon, n)$ is the reaction field factor [23], $T = 293$ K

Solvent	Cyclohexane	Decalin	Paraffin oil	Dioxane	Fluorobenzene	Tetrahydrofuran	DMSO
$F(\varepsilon, n)$	−0.002	0.001	0.004	0.021	0.157	0.209	0.263
FET							
I_{N^*}/I_{T^*}	–	0.002	0.012	0.027	0.039	0.097	0.640
ν_{em}^{max} (cm^{-1}), normal form	–	21 800	21 300	20 900	20 400	19 700	18 400
ν_{em}^{max} (cm^{-1}), phototautomer	–	17 500	17 500	17 300	17 400	17 200	16 800
FCR							
I_{N^*}/I_{T^*}	0.005	0.003	0.016	0.061	0.055	0.050	0.890
ν_{em}^{max} (cm^{-1}), normal form	22 700	22 500	22 100	21 400	20 800	20 300	18 900
ν_{em}^{max} (cm^{-1}), phototautomer	17 800	17 600	17 600	17 500	17 500	17 200	17 100

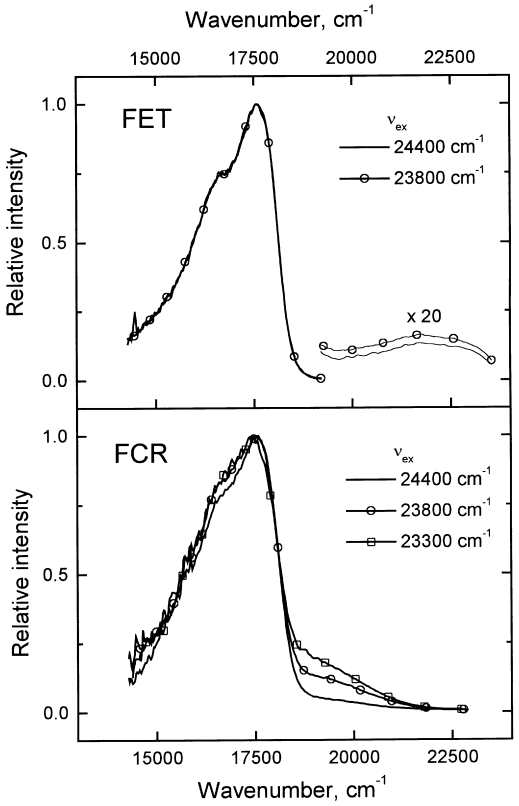

Fig. 5. Room temperature normalized fluorescence spectra of FET and FCR in decalin with volume concentrations of DMSO 2% excited by various frequencies: 24 400 cm^{-1} (—), 23 800 cm^{-1} (–○–), and 23 300 cm^{-1} (–□–). The emission spectrum of the normal form of FET expanded 20 times.

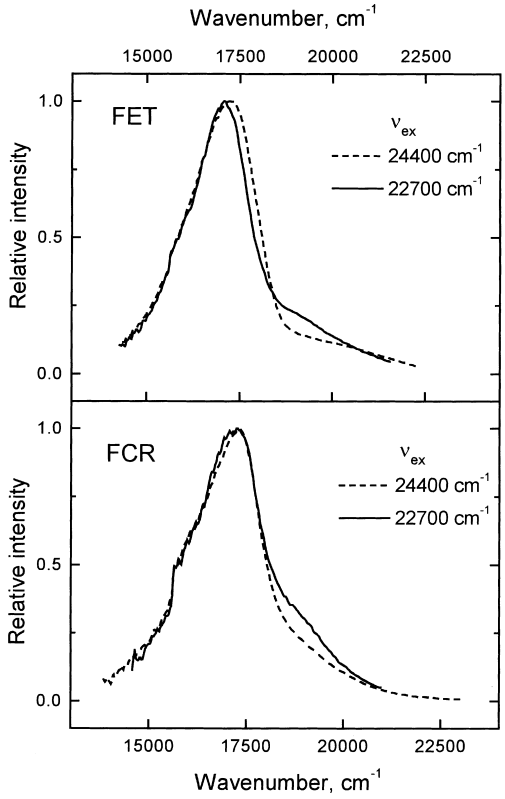

Fig. 6. Room temperature normalized fluorescence spectra of FET and FCR in hemoglobin-free ghosts of human erythrocytes excited by frequencies: 24 400 cm^{-1} (– – –) and 22 700 cm^{-1} (—).

The results we have obtained on the steady-state fluorescence measurements on FET and FCR in human erythrocyte ghosts show that the ratio I_{N^*}/I_{T^*} and the position of both the N^* and T^* emission bands depend on the excitation frequency, just as in binary solvents. The steady-state fluorescence spectra of FET and FCR in hemoglobin-free ghosts of human erythrocytes are presented in Fig. 6. The dashed and solid curves correspond to the excitation frequencies 24 400 and 22 700 cm^{-1}, respectively. As in the binary solvents, the fluorescence intensity of the normal form increases at red-edge excitation.

3.3. Electro-optical measurements

Table 2 gives the electro-optical coefficients obtained by EOAM for FET in dioxane at $T = 298$ K. All coefficients were measured with an accuracy of a few percent. As can be seen from Table 2, the coefficients H and I are equal to each other within the experimental error. This means that the vectors $\boldsymbol{m}_a$ and $\Delta^a\boldsymbol{\mu}$ are parallel. Taking this into account and assuming that all vectors lie in one plane, the values $\boldsymbol{\mu}_g$, $\Delta^a\boldsymbol{\mu}$, $\boldsymbol{\mu}_e{}^{FC}$ and the angles between different dipole moments of the normal form can be evaluated from the coefficients E, F, G, H and I using Eqs. (8)–(12). The results are shown in Table 3 and, as a vector diagram, in Fig. 1. The value and direction of the vector $\boldsymbol{\mu}_e{}^{FC}$ in the excited Franck–Condon state were found from the formula

$$\Delta^a\boldsymbol{\mu} = (\boldsymbol{\mu}_e{}^{FC} - \boldsymbol{\mu}_g) \quad (13)$$

which is valid in good approximation for non-polar solvents.

4. Discussion

4.1. Mechanism of charge and proton transfer in 4′-amino-3-hydroxyflavones

ESIPT in flavonols has been extensively studied both experimentally and theoretically [24–43]. The basic mechanism of ESIPT for flavonols in aprotic solvents is as fol-

Table 2
Electro-optical coefficients obtained by EOAM for FET in dioxane at $T = 298$ K

Coefficient	Value
E (10^{-20} V^{-2} m^2)	3440
F (10^{-40} C V^{-1} m^2)	2100
G (10^{-40} C V^{-1} m^2)	2150
H (10^{-60} C^2 m^2)	1720
I (10^{-60} C^2 m^2)	1740

Table 3
Dipole moments of the normal form of FET in dioxane at $T = 298\,K$[a]

μ_g (10^{-30} C m)	$\Delta^a\mu$ (10^{-30} C m)	$\boldsymbol{\mu}_e^{FC}$ (10^{-30} C m)	$\angle(\Delta^a\mu, \boldsymbol{m}_a)$	$\angle(\mu_g, \boldsymbol{m}_a)$	$\angle(\boldsymbol{\mu}_e^{FC}, \boldsymbol{m}_a)$	$\angle(\boldsymbol{\mu}_g, \boldsymbol{\mu}_e^{FC})$
22.7	34	53.3	0°	41°	16°	25°

[a] $\boldsymbol{\mu}_g$ is the dipole moment in the equilibrium ground state, $\Delta^a\boldsymbol{\mu}$ the change of the dipole moment vector after excitation to the Franck–Condon state, $\boldsymbol{\mu}_e^{FC}$ the dipole moment in the excited Franck–Condon state, and $\boldsymbol{m}_a$ the transition dipole moment.

lows. After optical excitation, the normal form (N*) undergoes ultrafast transfer of a proton from the hydroxyl group to the carbonyl oxygen (see Fig. 1), resulting in the appearance of a phototautomer emission band with a large Stokes shift. The most important feature of the derivatives of 3-hydroxyflavone studied in this work is significant charge separation for the normal form in the ground and excited electronic state as well as effective charge transfer after excitation. This follows from the large long-wavelength shift of the absorption and fluorescence spectra of the normal form with increasing solvent polarity (see Figs. 2–4 and Table 1) and in the case of FET, directly from electro-optical measurements (see Table 3). The electrical dipole moments of FET in the ground and excited Franck–Condon state have the values 22.7×10^{-30} and 53.3×10^{-30} C m, respectively. On optical excitation, the electric dipole moment increases by 34×10^{-30} C m, and the angle between $\boldsymbol{\mu}_g$ and $\boldsymbol{\mu}_e^{FC}$ is 25° within a relatively large error. The above values of the electrical dipole moments are much larger than for parent 3-hydroxyflavone [44].

As a result of the essential change of the dipole moment upon excitation, the polarity of the environment strongly affects the S_0–S_1 transition energy and position of the absorption and the fluorescence spectra of the normal form. On the other hand, the S_1–S_0 transition energy and position of the phototautomer fluorescence spectra are much less sensitive to the environment polarity (see Fig. 3). Thus, in the polar solvents, the relatively small energy difference for the S_1-state of the normal form compared to that of the phototautomer may lead to an increase in the probability of reverse ESIPT. From this point of view, an increase in the ratio of I_{N^*}/I_{T^*} in binary solvents with increasing concentration of polar additives, as obtained in this work, is not surprising. Actually, due to the large value of the electric dipole moment of the probe and strong dipole–dipole interactions, the molecules of the polar component in binary solvents are accumulated in the first solvate shell [23]. Hence, even small additions of polar solvents lead to a significant increase in the local polarity around the probe molecules and cause an increase in the ratio I_{N^*}/I_{T^*} (Fig. 4).

Another important point is the energy fluctuation of the probe interaction with the nearest molecules of the polar component. In binary solvents, the intermolecular interaction energy fluctuation is associated with the solvate composition and molecular configuration changes caused by the thermal molecular motion. The influence of such energy fluctuations on ESIPT is discussed below in Section 4.2.

The mechanism of proton and charge transfer in parent 3-hydroxyflavone and its 4′-amino derivatives has been repeatedly discussed in the scientific periodicals [12–16,25–34]. The results of EOAM and spectral measurements allow us to elucidate in more detail the mechanism of proton and charge transfer in the flavonols studied in this work. The amino-group in the side ring of 3-hydroxyflavone has a substantial influence on the π-electron density distribution in the ground S_0-state, and an even more stronger influence in the excited S_1-state. As a result, the spectral properties of 4′-amino derivatives differ significantly from the properties of the parent 3-hydroxyflavone. According to the quantum-chemical calculations performed in the manner described in Ref. [16], the π-electron density distribution in the S_0-state of 3-hydroxyflavone derivatives can be clearly described using two mesomeric structures N1 and N2, where the last structure plays the determining role (Fig. 7). Additionally, in 4′-amino-3-hydroxyflavones, structure N3 makes a perceptible contribution to the electron density distribution in the S_0-state. This is the result of the nitrogen's lone pair conjugation with the aromatic system of the whole molecule, which leads to partial charge transfer from the nitrogen to electron-deficient atoms. From the obtained values of the dipole moments and the angle between $\boldsymbol{\mu}_g$ and $\boldsymbol{\mu}_e^{FC}$, it follows that in the Franck–Condon S_1-state, structure N3 largely determines the total π-electron density distribution in the FET molecule. These data together with the steady-state spectroscopic data enable us to describe more precisely the processes taking place in 4′-amino-3-hydroxyflavones on optical excitation.

It can be supposed that after photon absorption, the ICT process occurs in the direction from the nitrogen atom to the carbonyl oxygen (process 1* in Fig. 7). This process is accompanied by a significant increase in the electric dipole moment. The ICT increases the basicity of the carbonyl oxygen, which leads to proton transfer from the hydroxyl to the carbonyl group. The phototautomer T* has a smaller electric dipole moment than N* because the centers of positive and negative charges in it are located closer to each other. Proton binding with carbonyl oxygen increases the deficit of the electron density on it. Thus, a further step of ICT process takes place after ESIPT (process 2* in Fig. 7). It should be noted that the oxygen in position 3, carrying a negative charge, cannot compensate for such an electron density shift because it is in cross-conjugation with the chromophore system of the molecule.

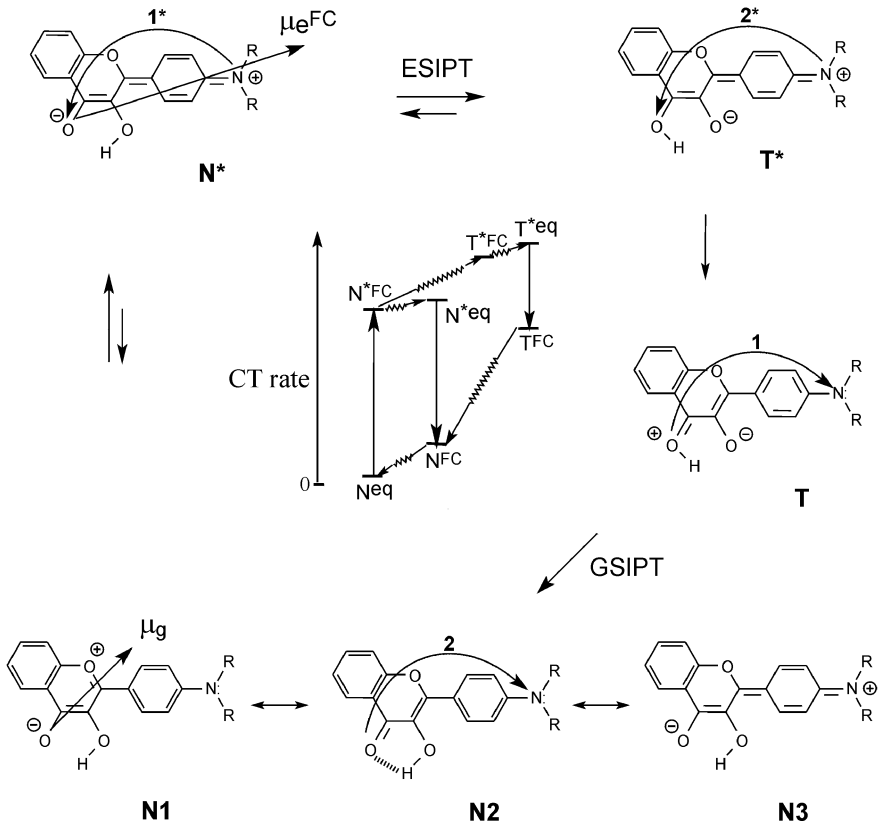

Fig. 7. Scheme of intramolecular charge and proton transfer in FET. The approximate change of the ICT rate is shown in the center (see explanation in text).

In solutions with low viscosity, photon emission preferably occurs from the relaxed states N^{*eq} and T^{*eq} (see diagram in Fig. 7). The substantially smaller solvatofluorochromic effect for the T^* band as compared to the N^* band points to a smaller change in the phototautomer dipole moment at its transition to the ground Franck–Condon state T^{FC}. Thus, for the form T only a small part of the reverse ICT is accompanied by photon emission. Actually, for the phototautomer, the return to the relaxed ground state N^{eq} consists of three ICT steps, and only step (1) takes place after photon emission. Step (2) is radiationless ground-state intramolecular proton transfer (GSIPT), which is accompanied by considerable reverse ICT since the carbonyl oxygen loses its electron withdrawing properties on deprotonation.

4.2. Interpretation of the red-edge excitation effects

In analyzing the spectral properties of fluorescent probes in liquid media, one must consider the nonspecific interactions (dipole–dipole, etc.) of the probe with the surrounding molecules or their segments. Due to the temperature fluctuations of solvate shells, built up around chemically identical probe molecules, different solvates do not have the same spatial structure, i.e., possess different free energy. This factor causes inhomogeneous broadening of the probe electronic spectra in pure and binary solvents [7,45]. In biological membranes, the inhomogeneous spectral broadening is of somewhat different nature [11,46]. As the incorporation of a fluorescent probe into the membrane is a statistical process, a certain distribution of the probe over location may take place. Therefore, different electric fields may be effective to molecules at different sites. This results in statistical variation of the energy of intermolecular interactions and, consequently, in inhomogeneous broadening of electronic spectra. Besides, at each location of the probe free energy fluctuations are possible due to the segmentary dynamics of biological macromolecules and due to a change in the magnitude and direction of the local electric field in the membrane.

Another important point is the possibility of selective excitation at the red edge of the absorption spectrum of a chosen group of probe molecules from an inhomogeneous ensemble [7,8]. Recent theoretical and experimental studies [47–56] of photochemical, electro-chemical and thermal charge (electron and proton) transfer reactions in polar solvents have revealed that the charge transfer rate is controlled by intermolecular relaxation and, in the adiabatic limit, is determined by the longitudinal dielectric relaxation time of the solvent. An important feature of solvent-controlled reactions is that the rate of charge transfer reactions may depend on the exciting light wavelength [57,58], because the efficiency of charge transfer depends critically on the initial conditions.

As mentioned in Section 3.2, selective excitation at the red edge of the absorption spectrum leads to an increase in the ratio I_{N^*}/I_{T^*} for the probe molecules in binary solvents and erythrocyte ghosts. Most likely, such an effect may be explained by selective excitation of certain groups of fluorescent molecules which interact with the environment more strongly. The probability of ESIPT for the molecules of these groups differs from the corresponding value averaged over the whole inhomogeneous ensemble. One may expect that in this situation, the relative probability of ESIPT as compared to ICT may change. An alternative explanation of the obtained results in terms of inhomogeneous spectral broadening may be based on the excitation of distinct ground-state conformers with a different probability of ESIPT. But this possibility must be considered very low in our case, because the excitation spectra of both emission bands are practically identical.

In our previous works [7,11,46], we proposed a free energy diagram for the description of effects of spectroscopic inhomogeneous broadening in polar solutions. The diagram describes the dependence of free energy of the probe-environment centers (solvates) on the local electric field strength R. The ground-state solvate free energy will be described by the following equation:

$$F_g(R) = \frac{(R - R_g^{eq})^2}{2\alpha} \quad (14)$$

where R_g^{eq} is the field strength in the equilibrium solvate, α the susceptibility of the solution determined by the Clausius–Mosotti formula [7].

The free energy of excited solvates is determined by a similar relation:

$$F_e(R) = \frac{(R - R_e^{eq})^2}{2\alpha} + h\nu_0 + \frac{\alpha}{2}(\boldsymbol{\mu}_e + \boldsymbol{\mu}_g)(\boldsymbol{\mu}_e - \boldsymbol{\mu}_g) \quad (15)$$

where ν_0 is the frequency of the pure electronic transition of the free probe molecule, h the Planck constant, $\boldsymbol{\mu}_g$ and $\boldsymbol{\mu}_e$ the dipole moments of the probe molecule in the equilibrium ground and excited states and R_e^{eq} is the local electric field corresponding to the equilibrium excited state of the solvate.

The field R in the solvates serves as a generalized coordinate, which describes the effect of the local microstructure of the surrounding medium on the fluorescent molecule. This parameter varies due to the fluctuation of the number and orientation of polar molecules (or in the case of biological membranes of their segments).

The same free energy diagram plotted for both the normal and phototautomer forms in a polar medium is shown in Fig. 8. This figure illustrates the excitation and fluorescence pathways of flavonols as well as ESIPT and GSIPT. Each point on the curves corresponds to a particular type of solvate with the field R. Since the field R has no time to change during the electronic transition (except for its electronic component, which can be ignored for polar solutions), electronic transitions are represented in the diagram by vertical arrows

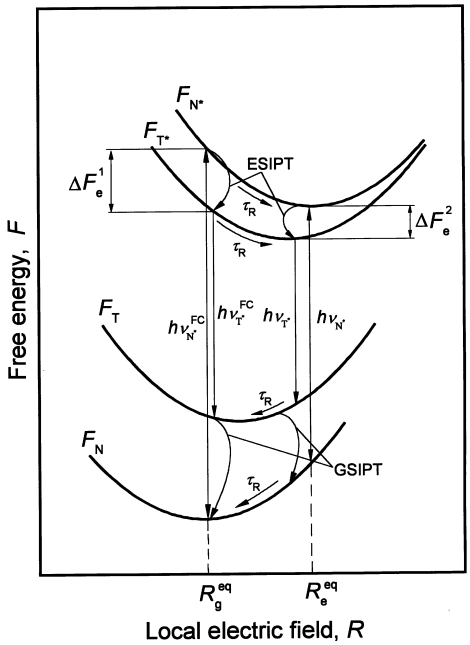

Fig. 8. Free energy diagrams plotted for the normal (F_{N,N^*}) and phototautomer (F_{T,T^*}) forms in polar aprotic media. This figure illustrates excitation and fluorescence pathways of flavonols as well as ESIPT and GSIPT. Each point on the curves corresponds to a particular type of fluorescent center (solvate) with the local electric field R (see explanation in text).

(intermolecular interpretation of the Franck–Condon principle). The field R also cannot change its value during ESIPT, because in aprotic solvents, the time of this process lies in the femtosecond range [39–41]. The diagram is given for the case where the electric dipole moments of both the normal form and phototautomer in the excited state are larger than in the ground state and the dipole moment of the phototautomer in the S_1-state is lesser than the dipole moment of the normal form in the excited state.

Let us consider the diagram (Fig. 8) to explain the red-edge excitation effects in binary solvents. In analyzing the diagram, it should be kept in mind that because of the relatively high viscosity of decalin (2.6 cP at $T = 293$ K) the configurational relaxation time τ_R in the mixture of decalin with polar additives is rather long (several nanoseconds [45,59]). Due to this, the process of intramolecular relaxation between different free energy sublevels for curves F_{N^*} and F_{T^*} does not complete during the excited-state lifetimes [1] of both forms. Also, as mentioned above, the characteristic time of ESIPT in flavonols is much shorter than their fluorescence lifetimes. In such a situation, the spectral heterogeneity of the probe molecules has a predominantly static character. Hence, when the excitation frequency corresponds to $h\nu_{N^*}{}^{FC}$ (the absorption spectrum maximum), ESIPT takes place primarily in the excited

[1] From our time-resolved measurements, it follows that fluorescence lifetimes of the normal form and phototautomer of FET and FCR vary from about 1 to about 5 ns depending on the medium (unpublished results).

Franck–Condon state of the normal form and the excess of the free energy in this case is equal to ΔF_e^1 (see Fig. 8). Fluorescence is emitted from the Franck–Condon states and from some of the intermediate nonrelaxed configurational sublevels of both the forms.

Analysis of the diagram shows that when the excitation frequency corresponds to $h\nu_{N^*}$ (red edge of the absorption spectrum), the process of ESIPT occurs in the excited equilibrium state of the normal form and the excess of the free energy in this case is equal to ΔF_e^2 (see Fig. 8). Fluorescence originates from the excited equilibrium state of the normal form and unrelaxed configurational sublevels of the phototautomer. Because $\Delta F_e^2 < \Delta F_e^1$, the probability of reverse ESIPT at excitation frequency $h\nu_{N^*}$ is higher than at frequency $h\nu_{N^*}{}^{FC}$. This effect is responsible for the increase in the ratio I_{N^*}/I_{T^*} at red-edge excitation. As follows from the diagram, a decrease in the excitation frequency to $h\nu_{N^*}$ (red edge of the absorption spectrum) should lead to a red shift of the steady-state fluorescence spectrum of the normal form.

It is likely that the proposed mechanism can also be used to explain the influence of the excitation frequency on the probability of ESIPT in erythrocyte ghosts. But at the moment, the possible role of intermolecular hydrogen bonding on ESIPT in such a system is not clear. This problem can be solved using time-resolved fluorescence measurements, which will be the subject of our future investigations.

5. Conclusions

Studies on FET and FCR have demonstrated different solvent sensitivity of the fluorescence spectra positions of the neutral form and phototautomer. As follows from our measurements, in polar aprotic solvents, the emission intensity ratio I_{N^*}/I_{T^*} increases with increasing solvent polarity. We have found that the addition of DMSO into neutral solutions of FET and FCR in decalin and paraffin oil leads to a significant increase in the fluorescence intensity of the normal form. The increase in the ratio between the normal and phototautomer emission intensities I_{N^*}/I_{T^*} in weakly polar and polar aprotic solvents and in binary solvents can be explained by the change in the rate of forward and reverse ESIPT and the interplay between charge and proton transfer.

The electric dipole moments of the normal form of FET in the ground and excited Franck–Condon states have the values 22.7×10^{-30} and 53.3×10^{-30} C m, respectively. On optical excitation, the electric dipole moment increases by 34×10^{-30} C m, and the angle between $\boldsymbol{\mu}_g$ and $\boldsymbol{\mu}_e{}^{FC}$ is roughly 25°.

The results of electro-optical and spectroscopic measurements allow us to describe more precisely the processes of charge and proton transfer in 4′-amino-3-hydroxyflavones. Charge and proton transfer occurs alternately. The main step of forward electron charge transfer takes place after the excitation of the normal form and partly after ESIPT. Additional shift of the electron density in the excited form N* may be described as the result of intermolecular relaxation in solution. In the phototautomer T, only partial reverse charge transfer happens after photon emission, which is responsible for its (T) small solvatofluorochromic effect. The second more significant stage of the reverse electron charge transfer occurs after the radiationless conversion of form T into form N.

The obtained results prove the existence of spectral heterogeneity of flavonols in binary solvents and in the hemoglobin-free ghosts of human erythrocytes. The effect of spectral inhomogeneity for flavonols manifests itself in the dependence of the ESIPT efficiency on the excitation frequency. The last phenomenon can be explained by the changes in the ratio between forward and reverse ESIPT on excitation at the red edge of the absorption spectrum.

Acknowledgements

This work was supported in part by the ISTC, Grant B-78 and partly by the Belarusian Republican Basic Research Foundation, Grant F97-309.

References

[1] J.R. Lakowicz, Principles of Fluorescent Spectroscopy, 2nd Edition, Plenum Press, New York, 1999.
[2] G.E. Dobretsov, Fluorescent Probes for Studying Cells, Membranes and Proteins, Nauka, Moscow, 1989 (in Russian).
[3] W. Rettig, W. Baumann, in: J.F. Ralek (Ed.), Progress in Photochemistry and Photophysics, Vol. VI, CRC Press, Boca Raton, FL, 1992, p. 79.
[4] W.R. Ware, S.R. Lee, G.I. Brand, P.P. Chow, J. Chem. Phys. 54 (1971) 4729.
[5] R.P. DeToma, J.H. Easter, L. Brand, J. Am. Chem. Soc. 98 (1976) 5001.
[6] L.A. Hallidy, M.R. Topp, Chem. Phys. Lett. 48 (1977) 40.
[7] N.A. Nemkovich, V.I. Tomin, A.N. Rubinov, in: J.R. Lakowicz (Ed.), Topic in Fluorescence Spectroscopy, Vol. 2, Principles, Plenum Press, New York, 1991, p. 367.
[8] A.P. Demchenko, Ultraviolet Spectroscopy of Proteins, Springer, Berlin, 1986.
[9] N.A. Nemkovich, A.N. Rubinov, V.I. Tomin, J. Lumin. 23 (1981) 349.
[10] A.D. Stein, K.A. Peterson, M.D. Fayer, Chem. Phys. Lett. 161 (1989) 16.
[11] D.M. Gakamsky, A.P. Demchenko, N.A. Nemkovich, A.N. Rubinov, V.I. Tomin, N.V. Shcherbatska, Biophys. Chem. 42 (1992) 49.
[12] P.-T. Chou, M.L. Martinez, J.H. Clements, J. Phys. Chem. 97 (1993) 2618.
[13] A. Sytnik, D. Gormin, M. Kasha, J. Fluoresc. 91 (1994) 11968.
[14] S.M. Ormson, R.G. Brown, F. Vollmer, W. Rettig, J. Photochem. Photobiol. A 81 (1995) 65.
[15] V.G. Pivovarenko, A.V. Tuganova, A.S. Klimchenko, A.P. Demchenko, Cell. Mol. Biol. Lett. 2 (1997) 355.
[16] A.D. Roshal, A.V. Grigorovich, A.O. Doroshenko, V.G. Pivovarenko, A.P. Demchenko, J. Phys. Chem. A 102 (1998) 5907.
[17] F.M. Dean, V. Podimuang, J. Chem. Soc. 7 (1965) 3978.
[18] M.A. Smith, R.M. Neumann, R.A. Webb, J. Heterocyclic Chem. 5 (1968) 425.

[19] J.A. Riddick, W.B. Bunger, T.K. Sakano, Organic Solvents, Wiley, New York, 1986.
[20] J.T. Dodge, C. Mitchell, D.J. Hanahan, Arch. Biochem. Biophys. 100 (1963) 119.
[21] W. Baumann, in: B.W. Rossiter, J.F. Hamitton (Eds.), Physical Methods of Chemistry, Vol. 3b, Wiley, New York, 1989, p. 45.
[22] W. Liptay, in: E.C. Lim (Ed.), Excited States, Vol. 1, Academic Press, New York, 1974, p. 129.
[23] N.G. Bakhshiev (Ed.), Solvatochromy: Problems and Methods, Leningrad University Press, Leningrad, 1989 (in Russian).
[24] Yu.L. Frolov, Yu.M. Sapozhnikov, N.N. Chipanina, V.F. Sidorkin, N. Tyukavkina, Izvestiya AN SSSR, Ser. Chim. 10 (1978) 301 (in Russian).
[25] P.K. Sengupta, M. Kasha, Chem. Phys. Lett. 68 (1979) 382.
[26] D. McMorrow, M. Kasha, J. Phys. Chem. 88 (1984) 2235.
[27] D. McMorrow, M. Kasha, Proc. Natl. Acad. Sci. USA 81 (1984) 3375.
[28] P. Chou, D. McMorrow, T.J. Aartsma, M. Kasha, J. Phys. Chem. 88 (1984) 4596.
[29] M. Kasha, J. Chem. Soc., Faraday Trans. 2 (82) (1986) 2379.
[30] M. Sarkar, P.K. Sengupta, Chem. Phys. Lett. 179 (1991) 68.
[31] A.J.G. Strandjord, P.F. Barbara, J. Phys. Chem. 89 (1985) 2355.
[32] A.J.G. Strandjord, D.E. Smith, P.F. Barbara, J. Phys. Chem. 89 (1985) 2362.
[33] M.C. Etter, Z. Urbanczyk-Lipkowska, S. Baer, P.F. Barbara, J. Mol. Struct. 144 (1986) 155.
[34] P.F. Barbara, P.K. Walsh, L.E. Brus, J. Phys. Chem. 93 (1989) 29.
[35] L. Vrielinck, G. Coustiller, J.P. Cornard, J.C. Merlin, in: P. Carmona, et al. (Eds.), Spectroscopy of Biological Molecules: Modern Trends, Kluwer Academic Publishers, Dordrecht, 1997, p. 141.
[36] L. Vrielinck, J.P. Cornard, J.C. Merlin, in: P. Carmona, et al. (Eds.), Spectroscopy of Biological Molecules: Modern Trends, Kluwer Academic Publishers, Dordrecht, 1997, p. 561.
[37] J.P. Cornard, L. Vrielinck, J.C. Merlin, in: P. Carmona, et al. (Eds.), Spectroscopy of Biological Molecules: Modern Trends, Kluwer Academic Publishers, Dordrecht, 1997, p. 563.
[38] G.J. Woolfe, P.J. Thistlethwaite, J. Am. Chem. Soc. 103 (1981) 6916.
[39] B.J. Shwartz, L.A. Peteanu, C. Harris, J. Phys. Chem. 95 (1992) 3591.
[40] G.A. Brucker, D.F. Kelley, J. Phys. Chem. 92 (1988) 3805.
[41] G.A. Brucker, T.C. Swinney, D.F. Kelley, J. Phys. Chem. 95 (1991) 3190.
[42] N.P. Ernsting, B. Dick, Chem. Phys. 136 (1989) 181.
[43] M. Itoh, Y. Fujiwara, M. Sumitani, K. Yoshihara, J. Phys. Chem. 90 (1986) 5672.
[44] L.V. Premvardhan, L.A. Peteanu, J. Phys. Chem. A 103 (1999) 7506.
[45] Yu.V. Zvinevich, N.A. Nemkovich, A.N. Rubinov, V.I. Tomin, J. Mol. Liquids 45 (1990) 1.
[46] N.A. Nemkovich, A.N. Rubinov, J. Fluoresc. 5 (1995) 285.
[47] E.M. Kosower, J. Am. Chem. Soc. 107 (1985) 1114.
[48] H. Sumi, R.A. Marcus, J. Chem. Phys. 84 (1986) 4272.
[49] B.S. Brunschwig, S. Ehrenson, N. Sutin, J. Phys. Chem. 90 (1986) 3657.
[50] J.T. Hynes, J. Phys. Chem. 90 (1986) 3701.
[51] I. Rips, J. Jortner, Chem. Phys. Lett. 133 (1987) 411.
[52] J.D. Simon, S.-G. Su, J. Chem. Phys. 87 (1987) 7016.
[53] M. Lee, J.T. Yardley, R.M. Hochstrasser, J. Phys. Chem. 91 (1987) 4621.
[54] R.I. Cukier, M. Morillo, J. Chem. Phys. 91 (1989) 857.
[55] T. Fonseca, J. Chem. Phys. 91 (1989) 2869.
[56] B. Bagchi, A. Chandra, G.R. Fleming, J. Phys. Chem. 94 (1990) 5197.
[57] A.P. Demchenko, A.I. Sytnik, Proc. Natl. Acad. Sci. USA 88 (1991) 9311.
[58] A.P. Demchenko, A.I. Sytnik, J. Phys. Chem. 95 (1991) 10518.
[59] Yu.V. Zvinevich, N.A. Nemkovich, A.N. Rubinov, J. Appl. Spectr. 58 (1993) 171.